Stabilizer Autopilot Design For Fixed Wing UAV Using ODSMC

Uygar GUNES[1], Artun SEL[2], Cosku KASNAKOGLU[3]
[1, 2, 3]Department of Electrical-Electronics Engineering
TOBB University of Economics and Technology
Ankara, Republic of Turkey
{[1]ggunes.uygar@gmail.com, [2]artunsel@gmail.com, [3]kasnakoglu@gmail.com}

Abstract— **In this paper we build an ODSMC (Output Feedback Discrete Time Sliding Mode Control) controller for a fixed-winged aircraft. ODSMC control is employed, which is widely utilized in commercial and reconnaissance applications. The small-disturbance theory is used to obtain the mathematical model of the system which has highly nonlinear and non-minimum characteristics. The ODSMC, due to its dynamic structure has been proved to be better than conventional linear controllers. Because of its output feedback structure, it also eliminates the need for a state observer. The ODSMC is designed based on the obtained linear model of the given plant. The effectiveness of the aircraft control system is analyzed by means of numerical simulations. The ODSMC control algorithm gives quite satisfactory results regarding the disturbance rejection capability of the closed loop system.**

Keywords—UAV; ODSMC.

I. INTRODUCTION

UAVs (Unmanned aerial vehicles) have gained popularity recently owing to the advancement in the manufacturing process of high torque generating motors and more efficient battery systems. The utilization of UAVs because of their efficiency compared to the conventional aircrafts and financial concerns have proven to be advantageous in both commercial and non-commercial application fields. One type of UAVs is fixed-winged aircraft which has traditionally 6 degrees of freedom dynamics [1]. Since the system does not have any rotating parts, their equations of motions are simpler to work with compared to the vehicles that have one or multiple rotating parts [2]. In addition to that, after employing small-disturbance theorem to obtain the linear system equations in a specified operating points, controller design process can be started [3]. It is important for the controller to be able to handle small disturbances which if not controlled can cause the system to diverge to a point which an employed control algorithm can no longer stabilize the system [4].

An output feedback discrete-time sliding mode control (ODSMC) is designed in this study for better robustness in face of the disturbances such as wind and change in atmospheric pressure.

Recently sliding mode control algorithms have proven to be quite useful for the highly coupled nonlinear plants and situations in which modelling errors might create unexpected problems [5]. ODSMC is a type of SMC (Sliding Mode Control) algorithm which is preferred specifically for reference tracking of the systems where invariant zeros are present. Since it is output feedback, unlike other nonlinear controllers such as feedback linearization technique [6] or linear control like LQR (Linear Quadratic Regulator), there is no need for state estimation [7].

The rest of the document is arranged as follows: Nonlinear plant model description and derivation of linear model using small-disturbance theorem is given in section II, controller mathematical model and determination of the key parameters is described in section III. Finally, to measure the performance of the controller, a series of scenarios concerning disturbances are simulated numerically.

II. SYSTEM MODELING

To design a controller it is of great importance to have a mathematical model of the system. The fixed-wing UAV is a significantly complicated system to be modelled considering all of the external forces and torques that also depend on the shape of the vehicle [8]. However, over the years under some assumptions which is discussed in this section that have proved to be valid have led to the model that is used in this paper [9].

An aircraft has conventionally 6 degrees of freedom dynamics, 3 torques and 3 forces govern the motion of an airplane. Due to aerodynamic and gravitational forces and torques, there are 3 translational and 3 angular velocities. This is illustrated in the Fig. 1[10].

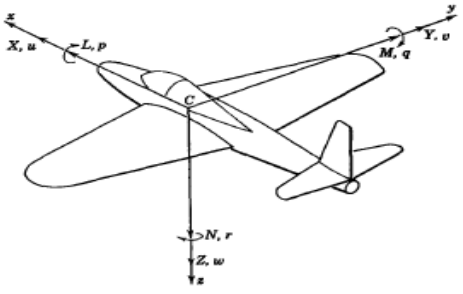

Fig. 1 Fixed-wing aircraft and Translational and Rotational Forces and Speeds.

u, v, w in Fig.1 are the translational velocities in the body reference frame. Additionally, if the effect of the wind is omitted, these speeds are equal to their earth reference frame counterparts. The roll, pitch and yaw angular speeds are denoted by p, q, r respectively. X, Y, Z denote translational forces and K, L, M represents angular forces that act on the aircraft in the axes as illustrated in the Fig. 1. Under the flat non-rotating earth assumptions, for a single rigid body that is symmetric about zx plane the equations that describe the motion are given as,

$$X - mg\sin\theta = m(\dot{u} + qw - rv) \tag{1}$$

$$Y + mg\cos\theta\sin\phi = m(\dot{v} + ru - pw) \tag{2}$$

$$Z + mg\cos\theta\cos\phi = m(\dot{w} + pv - qu) \tag{3}$$

$$L = I_x\dot{p} - I_{zx}\dot{r} + qr\left(I_z - I_y\right) - I_{zx}pq \tag{4}$$

$$M = I_y\dot{q} + rp(I_x - I_z) + I_{zx}(p^2 - r^2) \tag{5}$$

$$N = I_z\dot{r} - I_{zx}\dot{p} + pq\left(I_y - I_x\right) + I_{zx}qr \tag{6}$$

$$p = \dot{\phi} - \dot{\psi}\sin\theta \tag{7}$$

$$q = \dot{\theta}\cos\phi + \dot{\psi}\cos\theta\sin\phi \tag{8}$$

$$r = \dot{\psi}\cos\theta\cos\phi - \dot{\theta}\sin\phi \tag{9}$$

$$\dot{\phi} = p + (q\sin\phi + r\cos\phi)\tan\theta \tag{10}$$

$$\dot{\theta} = q\cos\phi - r\sin\phi \tag{11}$$

$$\dot{\psi} = (q\sin\phi + r\cos\phi)\sec\theta \tag{12}$$

$$\dot{x}_E = uc\theta c\psi + v(s\phi s\theta c\psi - c\phi s\psi) + w(c\phi s\theta c\psi + s\phi s\psi) \tag{13}$$

$$\dot{y}_E = uc\theta s\psi + v(s\phi s\theta s\psi + c\phi c\psi) + w(c\phi s\theta s\psi - s\phi c\psi) \tag{14}$$

$$\dot{z}_E = -us\theta + vs\phi c\theta + wc\phi c\theta \tag{15}$$

where ϕ, θ, ψ are Euclidian angles; I_x, I_y, I_z, I_{zx} are torque of inertias with respect to their axes. The terms c and s represents $\cos(\cdot)$ and $\sin(\cdot)$ in (13),(14) and (15). Under the assumptions that are mentioned, the above equations are quite reasonable to work. However, since the highly-coupled and nonlinear terms that are present in the model, further simplifications are required [11], [12]. For this need the small-disturbance theory is applied. The small-disturbance theory is common for nonlinear system linearization especially in power electronic circuit modeling [13].

Every state is composed of a steady state component and a small-perturbation deviated from the steady state and it is given as,

$$x = x_0 + \Delta x \tag{16}$$

Since the small signal component is much smaller compared to the steady state component, the multiplications of small signal components of the state variables are assumed to be zero [14]. This fundamental assumption leads to a reasonable model. After applying the described method, the equations are simplified to,

$$\Delta\dot{u} = \frac{\Delta X}{m} - g\Delta\theta\cos\theta_0 \tag{17}$$

$$\dot{v} = \frac{\Delta Y}{m} + g\phi\cos\theta_0 - u_0 r \tag{18}$$

$$\dot{w} = \frac{\Delta Z}{m} - g\Delta\theta\sin\theta_0 + u_0 q \tag{19}$$

$$\dot{p} = (I_x I_z - I_{xz}^2)^{-1}(I_z\Delta L + I_{xz}\Delta N) \tag{20}$$

$$\dot{q} = \frac{\Delta M}{I_y} \tag{21}$$

$$\dot{r} = (I_x I_z - I_{xz}^2)^{-1}(I_{zx}\Delta L + I_x\Delta N) \tag{22}$$

$$\Delta\dot{\theta} = q \tag{23}$$

$$\dot{\phi} = p + r\tan\theta_0 \tag{24}$$

$$\dot{\psi} = r\sec\theta_0 \tag{25}$$

$$\Delta\dot{x}_E = \Delta u\cos\theta_0 - u_0\Delta\theta\sin\theta_0 + w\sin\theta_0 \tag{26}$$

$$\Delta\dot{y}_E = u_0\psi\cos\theta_0 + v \tag{27}$$

$$\Delta\dot{z}_E = -\Delta u\sin\theta_0 - u_0\Delta\theta\cos\theta_0 + w\cos\theta_0 \tag{28}$$

for each variable whose steady state component is zero, the Δ notation is dropped. Additionally, the small signal components of the forces and torques that act on the plane are given as,

$$\Delta X = X_u\Delta u + X_w w + \Delta X_c \tag{29}$$

$$\Delta Y = Y_v v + Y_p p + Y_r r + \Delta Y_c \tag{30}$$

$$\Delta Z = Z_u\Delta\mathrm{u} + \mathrm{Z_w}w + \mathrm{Z_{\dot{w}}}\dot{w} + Z_q q + \Delta Z_c \tag{31}$$

$$\Delta L = L_v v + L_p p + L_r r + \Delta L_c \tag{32}$$

$$\Delta M = M_u\Delta u + M_w w + M_{\dot{w}}\dot{w} + M_q q + \Delta M_c \tag{33}$$

$$\Delta N = N_v v + N_p p + N_r r + \Delta N_c \tag{34}$$

where each variable subscripted with "c" expresses the control signal. The plant has 4 inputs that can be manipulated by the controller. They are elevator, aileron, rudder and propulsion force which are denoted as $\delta_e, \delta_a, \delta_r, \delta_p$, respectively. The other terms such as $X_u, X_w, Z_{\dot{w}}$ etc. are known to be stability derivatives of the airplane. The determination of those parameters is carried out either with the help of fluid dynamics simulations or wind tunnel

experimental studies [15], [16]. The control components of the forces and torques are given as,

$$\Delta X_c = X_{\delta_e}\Delta\delta_e + X_{\delta_p}\Delta\delta_p \quad (35)$$

$$\Delta Y_c = Y_{\delta_a}\Delta\delta_a + Y_{\delta_r}\Delta\delta_r \quad (36)$$

$$\Delta Z_c = Z_{\delta_e}\Delta\delta_e + Z_{\delta_p}\Delta\delta_p \quad (37)$$

$$\Delta L_c = L_{\delta_a}\Delta\delta_a + L_{\delta_r}\Delta\delta_r \quad (38)$$

$$\Delta M_c = M_{\delta_e}\Delta\delta_e + M_{\delta_p}\Delta\delta_p \quad (39)$$

$$\Delta N_c = N_{\delta_e}\Delta\delta_e + N_{\delta_p}\Delta\delta_p \quad (40)$$

In this study the system has 4 inputs, 12 states and 4 outputs and are given as,

$$x = [\Delta V\ \Delta\alpha\ \ \Delta\beta\ \ p\ \ q\ \ r\ \ \psi\ \ \Delta\theta\ \ \phi\ \ \Delta x_E\ \ \Delta y_E\ \ \Delta z_E]^T \quad (41)$$

$$u = [\Delta\delta_p\quad \Delta\delta_e\quad \Delta\delta_a\quad \Delta\delta_r]^T \quad (42)$$

$$y = [\Delta V\quad \Delta\beta\quad \Delta\theta\quad \phi]^T \quad (43)$$

where $\Delta V, \Delta\alpha, \Delta\beta$ are respectively the speeds of the aircraft in earth reference frame, the angle of attack and the sideslip angle. Their mathematical descriptions are given as,

$$\Delta V = (\Delta u^2 + \Delta v^2 + \Delta w^2)^{1/2} \quad (44)$$

$$\Delta\beta = \sin^{-1}\left(\frac{\Delta v}{\Delta V}\right) \quad (45)$$

$$\Delta\alpha = \tan^{-1}\left(\frac{\Delta w}{\Delta u}\right) \quad (46)$$

The numerical values of the steady state parts of the states, also known as operating point which is obtained under trim conditions of $V = 18.9\ m/s$ and the altitude of $1000\ m$. The operating point for the Apprentice S model aircraft is given in the TABLE I.

TABLE I. STATE VALUES AT OPERATING POINT

V	$18.9\ m/s$	p	$8.2x10^{-23}\ rad/s$	ψ	$7.4x10^{-19}\ rad$
α	$-0.02\ rad$	q	$4.9x10^{-23}\ rad/s$	θ	$-0.02\ rad$
β	$2.4x10^{-4}\ rad$	r	$-6.2x10^{-22} rad/s$	ϕ	$7.8x10^{-19}\ rad$
x_E	$1.2x10^{-15}\ m$	y_E	$0\ m$	z_E	$1000\ m$

III. CONTROLLER DESIGN

SMC is a control algorithm which is robust to the parameter uncertainty. It achieves that by employing a discontinuous function such as signum. This instantaneous change in the actuator signal causes chattering around the sliding surface. To overcome this, a boundary layer around the surface is constructed by employing a sigmoidal function. Another problem of SMC is that the plant needs to be minimum phase as well as have relative degree one. This restriction can be circumvented by employing a discrete time control scheme. Due to a discrete time control strategy, lower limit on sampling period creates a boundary layer. ODSMC is one of the discrete time control schemes and only consists of linear operations unlike SMC which also has nonlinear operation. ODSMC and its design process is addressed below.

Let the discrete time system be as follows

$$x_p(k+1) = G_p x_p(k) + H_p\big(u(k) + \xi(k)\big) \quad (47)$$

$$y(k) = C_p x_p(k) \quad (48)$$

where $x_p \in \mathbb{R}^n, u \in \mathbb{R}^m, y \in \mathbb{R}^p$. In this system, $G_p \in \mathbb{R}^{nxn}$, $H_p \in \mathbb{R}^{nxm}$ and $C_p \in \mathbb{R}^{pxn}$ represent system state, input and output distribution matrices respectively. Additionally, $\xi(k)$ represents matched uncertainties which is unknown but assumed to be bounded.

For the control law used in the paper, nonsingularity of G_p and rank of the matrix $C_p G_p^{-1} H_p$ equals to m assumptions are needed [17].

It is necessary to introduce some transformation for further analysis. A new output distribution matrix $L \coloneqq CG^{-1}$ is defined for the fictitious system represented by the (G, H, L) system matrices [18]. To distinguish the controllable states from the uncontrollable ones, the following transformation is performed on the system. System matrices of the resulting system can be partitioned as,

$$G = \begin{bmatrix} G_{11} & G_{12} \\ G_{21} & G_{22} \end{bmatrix}, H = \begin{bmatrix} 0 \\ H_2 \end{bmatrix}, L = [0 \quad T] \quad (49)$$

Where $G_{11} \in \mathbb{R}^{(n-m)x(n-m)}, H_2 \in \mathbb{R}^{mxm}$ and $T \in \mathbb{R}^{pxp}$ which is an orthogonal matrix [19]. The state vector in this coordinate is partitioned as $x = [x_1 \quad x_2]^T$.

Before introducing output feedback SMC control law, mentioning state feedback SMC will be proper. The aim of the SMC is to build a controller that drives the system states into a set and forces them stay in that set despite the disturbances that are considered to be bounded [20]. This set in state space is called sliding manifold and is represented by,

$$\mathcal{S} = \{x_p \in \mathbb{R}^n : H_p^T P x_p = 0\} \quad (50)$$

where $P \in \mathbb{R}^{nxn}$ is a symmetric positive definite matrix. This is used to define the system Lyapunov function which is given by,

$$V(k) = x_p(k)^T P x_p(k). \quad (51)$$

However, states may not be readily available for all circumstances. Additionally, designing a state feedback controller requires some complicated transformations for the plants that are non-minumum phase. Considering these

reasons, it is desirable to employ some type of an output feedback controller algorithm as stated in [21]. For the output feedback controller design, an additional constraint is imposed on the system and is given as,

$$H^T PG = FC \tag{52}$$

where $F \in \mathbb{R}^{mxm}$ and $P \in \mathbb{R}^{mxm}$ is a symmetric positive definite matrix used to construct the Lyapunov function to prove finite time convergence. (52) is required to be satisfied to prove that the states can be forced to the sliding surface by only using the knowledge of outputs alone under certain circumstances. However, there are certain classes of systems in which G_{11} is not Hurwitz, if so it is not possible to ensure the stability of the states that are not directly observable. To overcome this problem, additional dynamics or compensator must be considered [22].

In addition to the compensator dynamics, since this case is analyzed as a reference tracking problem, steady state error term must be kept zero. From this necessity, an integrator is added to the design procedure. The integral action dynamic equation is given by,

$$x_r(k+1) = x_r(k) + T_s\left(r(k) - C_p x_p(k)\right) \tag{53}$$

Due to the involvement of additional integrator and compensator dynamics, state vector x_p is extended and the problem dimension is increased. This new problem yields a new augmented system whose corresponding sliding manifold is represented as,

$$\mathcal{S}_a = \{(x_1, x_c, x_2, x_r): K_1 x_c + K_r x_r + x_2 + S_r r_s = 0\} \tag{54}$$

where $K_1 \in \mathbb{R}^{mx(n-m)}$, $K_r \in \mathbb{R}^{mxm}$ and $S_r \in \mathbb{R}^{mxm}$ represent design parameters related to the sliding surface.

The compensator dynamics are given by,

$$x_c(k+1) = \Phi x_c(k) + \Gamma_1 y_p(k) + \Gamma_2 x_r(k) + \Gamma_3 r(k) \tag{55}$$

where Φ, Γ_1, Γ_2 and Γ_3 represent the parameters of the compensator and are given explicitly by,

$$\Phi = G_{11} - \Omega T G_{21} - G_{21}K_1 + LTG_{22}K_1 \tag{56}$$

$$\Gamma_1 = \Omega \tag{57}$$

$$\Gamma_2 = -G_{12}K_r + \Omega T G_{22} K_r \tag{58}$$

$$\Gamma_3 = -G_{12}S_r + \Omega T G_{22} S_r \tag{59}$$

where Γ_1, Γ_2, Γ_3 and Φ are found depending on the surface parameters giving in (54). Dynamics of the augmented system are given by,

$$x_a(k+1) = G_a x_a(k) + H_a\big(u(k) + \xi(k)\big) + H_r r(k) \tag{60}$$

$$y_a(k) = C_a x_a(k) \tag{61}$$

Where G_a, H_a, H_r and C_a are the system matrices of the augmented system, after arranging the terms are found to be,

$$G_a = \begin{bmatrix} G_{11} & 0 & 0 & G_{12} \\ \Gamma_1 T G_{21} & \Phi & \Gamma_2 & \Gamma_1 T G_{22} \\ -T_s T G_{21} & 0 & I_m & -T_s T G_{22} \\ G_{21} & 0 & 0 & G_{22} \end{bmatrix}, H_a = \begin{bmatrix} 0 \\ 0 \\ 0 \\ H_2^T \end{bmatrix}$$
$$H_r = \begin{bmatrix} 0 \\ \Gamma_3 \\ T_s I_m \\ 0 \end{bmatrix}, C_a = \begin{bmatrix} 0 & I_{n-m} & 0 & 0 \\ 0 & 0 & I_m & 0 \\ TG_{21} & 0 & 0 & TG_{22} \end{bmatrix} \tag{62}$$

The control law for this augmented system is given by,

$$u(k) = -(FC_a G_a^{-1} H_a)^{-1}\big(FC_a x_a(k) + (FC_a G_a^{-1} H_r + F_2 S_r) r(k)\big) \tag{63}$$

where F is chosen dependent on the surface parameters given in (54) so as to stabilize the closed loop system. The eigenvalues of the closed loop system matrix denoted by G_c lies inside the unit circle when stability is achieved [23].

The design of the controller constitutes a problem of determination of the parameters F and P_a that satisfy the constraint defined for the augmented system. Sliding surface constraint for the augmented system is given by,

$$FC_a = H_a^T P_a G_a \tag{64}$$

where $P_a \in \mathbb{R}^{(2n-m+p)x(2n-m+p)}$ is a Lyapunov symmetric positive definite matrix and satisfies the Lyapunov constraint which is defined as,

$$P_a - G_c^T P_a G_c > 0 \tag{65}$$

Considering the surface constraint equation in (64), F is in the form given by,

$$F = F_2[K_1 \Phi \;\; (K_1\Gamma_2 + K_r) \;\; (K_1\Gamma_1 - K_r T_s + T^T)] \tag{66}$$

where $F_2 \in \mathbb{R}^{mxm}$ is a parameter that is chosen such that the constraint given in (64) is satisfied.

It is required to represent augmented system in another coordinate system for simplifying the design parameters K_1, K_r, Ω. For this operation, the transformation matrix is given by,

$$\tilde{T} = \begin{bmatrix} I_{n-m} & -I_{n-m} & 0 & 0 \\ 0 & I_{n-m} & 0 & 0 \\ 0 & 0 & I_m & 0 \\ 0 & K_1 & K_r & I_m \end{bmatrix} \tag{67}$$

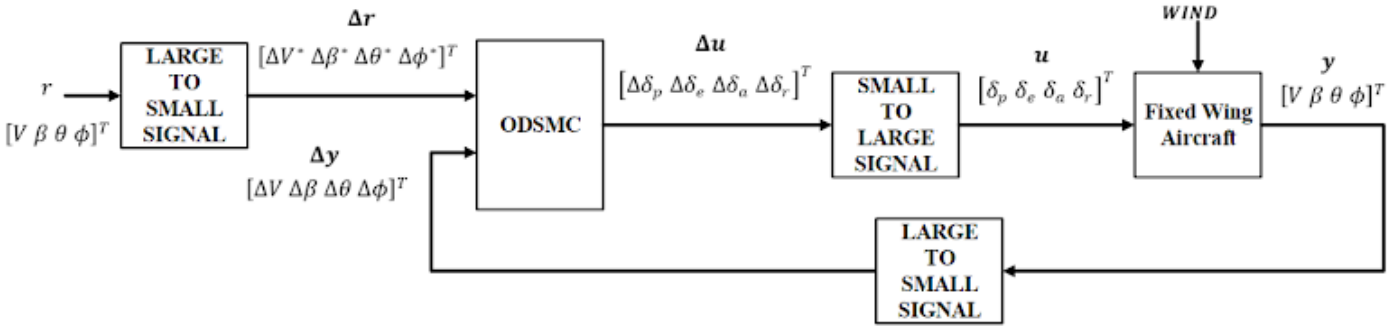

Fig. 2. ODSMC controlled system block diagram

The resulting system matrices are $\tilde{G} = \tilde{T}G_a\tilde{T}^{-1}$ $\tilde{H} = \tilde{T}H_a, \tilde{H}_r = \tilde{T}H_r, \tilde{C} = C_a\tilde{T}^{-1}$ and $\tilde{L} = L_a\tilde{T}^{-1}$[24].

Using the control law given in (63), the closed loop system matrix is given by,

$$\tilde{G}_c \coloneqq \tilde{G} - \tilde{H}\left(F\tilde{L}\tilde{H}\right)^{-1}F\tilde{C} \tag{68}$$

where $\tilde{G}_c$ has the structure and given by,

$$\tilde{G}_c \coloneqq \begin{bmatrix} G_{11} - \Omega T G_{21} & 0 & * \\ * & \tilde{G}_m & * \\ 0 & 0 & 0 \end{bmatrix} \tag{69}$$

Inferred from (69), the eigenvalues of $\tilde{G}_c$ must lie inside the unit circle.

Due to the special structure of $\tilde{T}$, by inspection, the closed loop matrix has the following eigenvalues

$$\lambda\left(\tilde{G}_c\right) = \{0\}^m \cup \lambda(G_{11} - \Omega T G_{21}) \cup \lambda\left(\tilde{G}_m\right) \tag{70}$$

where $\tilde{G}_m$ is given by,

$$\tilde{G}_m = \begin{bmatrix} G_{11} & 0 \\ -T_s T G_{21} & I_m \end{bmatrix} - \begin{bmatrix} G_{12} \\ -T_s T G_{22} \end{bmatrix} [K_1 \quad K_r] \tag{71}$$

It is clear from (71) the parameters K_1 and K_r are chosen such that $\left|\lambda_{max}\left(\tilde{G}_m\right)\right| < 1$. Likewise, Ω matrix is determined such that $|\lambda_{max}(G_{11} - \Omega T G_{21})| < 1$. In the process of choosing the new pole locations, the old locations of the poles were taken into account not to place the poles too far from their own old locations. "lqr" which is a numerically stable robust pole placement algorithm of MATLAB was used.

Lastly in this new coordinate system, Lyapunov matrix $\tilde{P}$ has the block diagonal form that is given by,

$$\tilde{P} = \begin{bmatrix} \tilde{P}_1 & 0 \\ 0 & \tilde{P}_2 \end{bmatrix} \tag{72}$$

And is constrained for the system in this coordinates by the equation,

$$\tilde{H}^T\tilde{P}\tilde{G} = F\tilde{C} \tag{73}$$

where $\tilde{P}_1 \in \mathbb{R}^{(2n-m)x(2n-m)}$ and $\tilde{P}_2 \in \mathbb{R}^{mxm}$. By some algebraic manipulation,

$$F_2 = H_2\tilde{P}_2 \tag{74}$$

Thus the controller design is completed [25]. Fig 2. presents a block diagram summarizing the control scheme.

IV. Simulation Results

In this study, the Apprentice S model aircraft is modeled and ODSMC is designed. The numerical values of the system matrices of the plant linearized around the operating points that are given in the TABLE I.

The Ω matrix is chosen such that the poles of the matrix $(G_{11} - \Omega T G_{21})$ is given as,

$$\lambda(G_{11} - \Omega T G_{21}) = \{0.9076, 0.998, 0.0005, 0.3482 \pm 0.0118j\} \tag{75}$$

The $[K_1 \quad K_r]$ matrix is determined so that the $\lambda\left(\tilde{G}_m\right)$ is given as,

$$\lambda\left(\tilde{G}_m\right) = \{0.9852, 0.8052, 0.7679, 0.3107, -0.2585, 0.0057, 0.0056, -0.0011, 0.0001\} \tag{76}$$

During the nominal operation, the wind is applied to disturb the plant in all three direction as given in the Fig. 3.

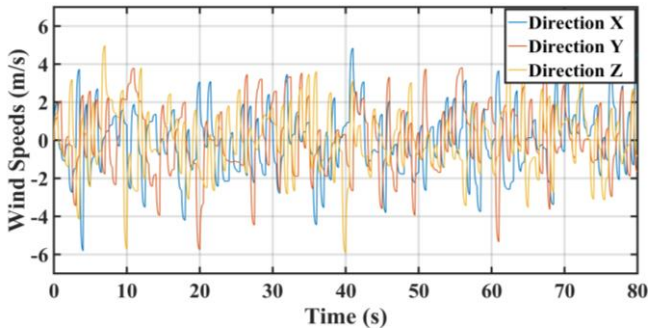

Fig. 3. Wind speeds

To simulate the effects of sensor noise, white noises were applied to V, β, θ and ϕ outputs with maximum amplitude of 0.1, 0.2, 0.3 and 0.25.

In the simulations, 4 outputs, $[V \quad \beta \quad \theta \quad \phi]^T$,which are given reference values as illustrated in the Fig. 4-Fig. 7. As illustrated in the figures the output variables track the reference values that are assigned.

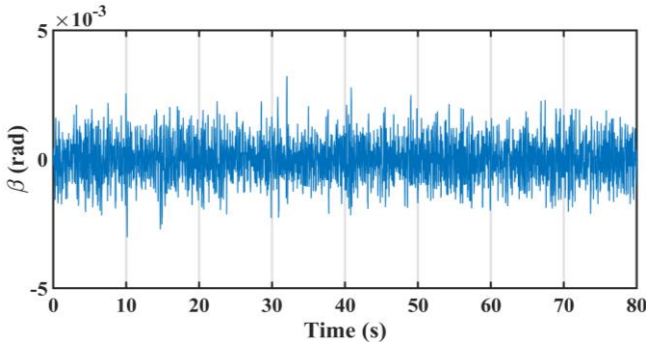

Fig. 4. Output sideslip angle

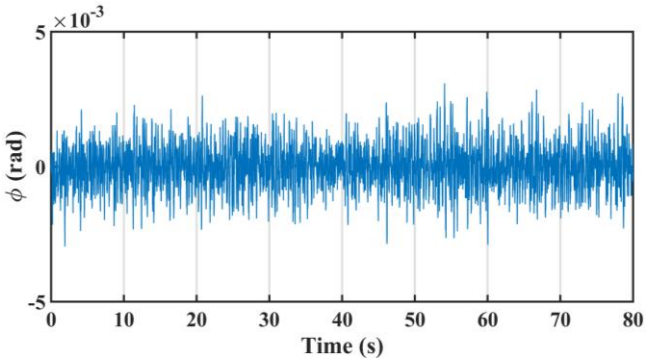

Fig. 5. Output roll angle

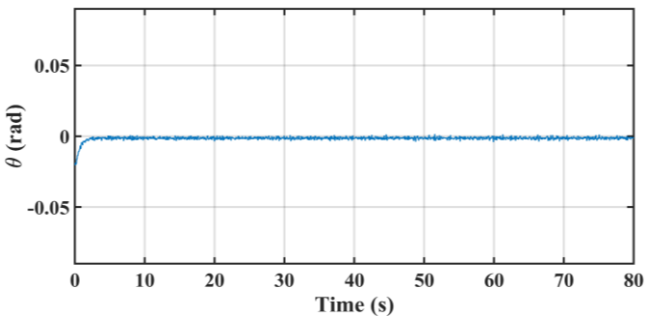

Fig. 6. Output pitch angle

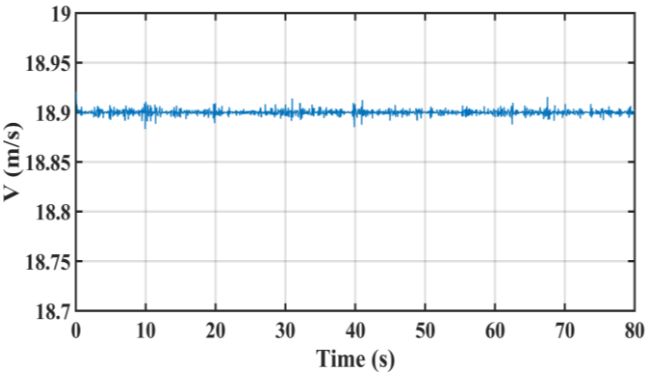

Fig. 7. Output speed

The actuator signals $[\delta_p \quad \delta_e \quad \delta_a \quad \delta_r]^T$ are given in the Fig. 8-Fig. 11.

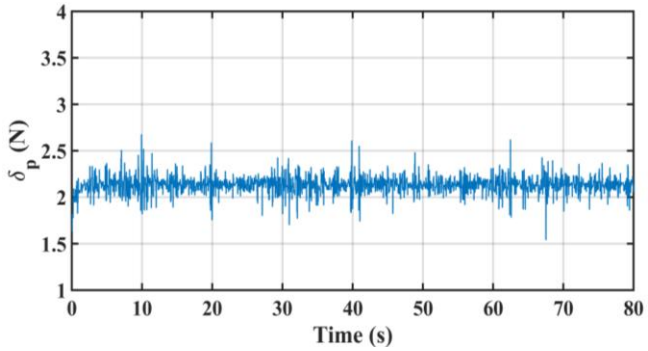

Fig. 8. Controller propulsion output

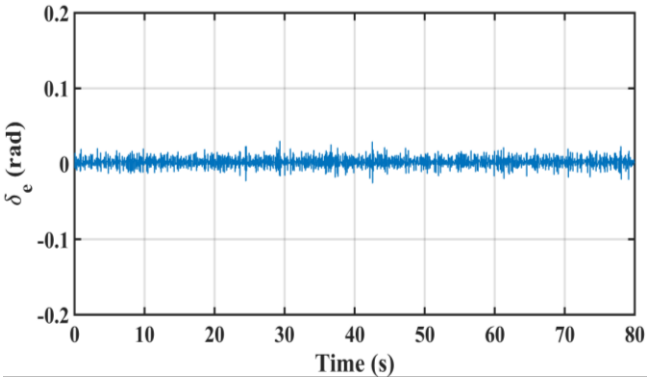

Fig. 9. Controller elevator output

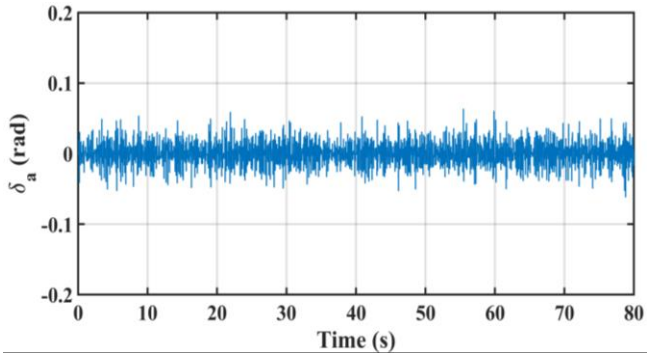

Fig. 10. Controller aileron output

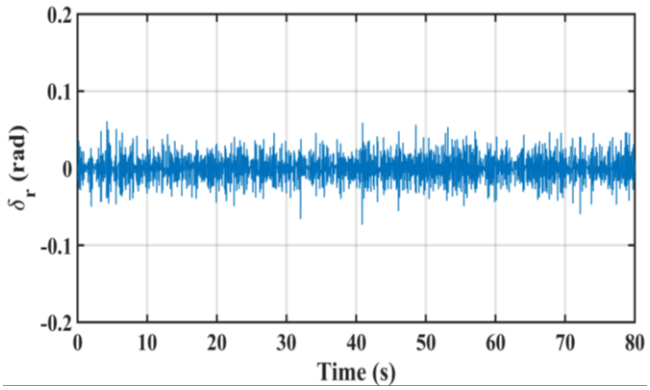

Fig. 11. Controller rudder output

V. CONCLUSIONS

This study first models the Apprentice S fixed wing aircraft by using small signal modeling. Based on that mathematical model linearized around the operating points of the plant, the ODSMC is designed for the system. The effectiveness of the output feedback SMC is seen through simulations carried out in Matlab/SIMULINK environment. As seen from the simulation results considerable disturbance rejection is achieved.

Our research group is currently working on real flight tests using novel controller design approaches for multiple trim conditions.

ACKNOWLEDGMENT

The authors thank the Scientific and Technological Research Council of Turkey (TÜBİTAK) for supporting this study under grant number 116E187.

REFERENCES

[1] S. H. Mathisen, T. I. Fossen and T. A. Johansen, "Non-linear model predictive control for guidance of a fixed-wing UAV in precision deep stall landing," 2015 International Conference on Unmanned Aircraft Systems (ICUAS), Denver, CO, 2015, pp. 356-365.J. Clerk Maxwell, A Treatise on Electricity and Magnetism, 3rd ed., vol. 2. Oxford: Clarendon, 1892, pp.68-73.

[2] Y. Kang and J. K. Hedrick, "Linear Tracking for a Fixed-Wing UAV Using Nonlinear Model Predictive Control," in *IEEE Transactions on Control Systems Technology*, vol. 17, no. 5, pp. 1202-1210, Sept. 2009.

[3] M. Żugaj, "Reconfiguration of fixed-wing UAV control system in autonomous flight," *2017 22nd International Conference on Methods and Models in Automation and Robotics (MMAR)*, Miedzyzdroje, 2017, pp. 1063-1068.

[4] S. Akyurek, U. Gunes, O. Elbir, C. Kasnakoglu and U. Kaynak, "Rudder loss recovery autopilot system for a small fixed-wing aircraft," 2017 10th International Conference on Electrical and Electronics Engineering (ELECO), Bursa, 2017, pp. 752-757

[5] Y. Shen, "Research on chattering and limit cycle adjusting for output feedback SMC based on frequency domain analysis," *The 26th Chinese Control and Decision Conference (2014 CCDC)*, Changsha, 2014, pp. 2465-2469.

[6] Z. Wu, Y. Shen, T. Pan and Z. Ji, "Feedback linearization control of PMSM based on differential geometry theory," 2010 5th IEEE Conference on Industrial Electronics and Applications, Taichung, 2010, pp. 2047-2051.

[7] M. A. M. Cheema, J. E. Fletcher, D. Xiao and M. F. Rahman, "A Linear Quadratic Regulator-Based Optimal Direct Thrust Force Control of Linear Permanent-Magnet Synchronous Motor," in IEEE Transactions on Industrial Electronics, vol. 63, no. 5, pp. 2722-2733, May 2016.

[8] M. G. Michailidis, K. Kanistras, M. Agha, M. J. Rutherford and K. P. Valavanis, "Robust nonlinear control of the longitudinal flight dynamics of a circulation control fixed wing UAV," 2017 IEEE 56th Annual Conference on Decision and Control (CDC), Melbourne, VIC, 2017, pp. 3920-3927.

[9] S. Akyurek, G. S. Ozden, B. Kurkcu, U. Kaynak and C. Kasnakoglu, "Design of a flight stabilizer for fixed-wing aircrafts using H∞ loop shaping method," 2015 9th International Conference on Electrical and Electronics Engineering (ELECO), Bursa, 2015, pp. 790-795

[10] Etkin, B., & Reid, L. D. (1996). Dynamics of flight: Stability and control. New York: Wiley.

[11] T. A. Johansen, A. Cristofaro, K. Sørensen, J. M. Hansen and T. I. Fossen, "On estimation of wind velocity, angle-of-attack and sideslip angle of small UAVs using standard sensors," 2015 International Conference on Unmanned Aircraft Systems (ICUAS), Denver, CO, 2015, pp. 510-519.

[12] E. de Souza Goncalves and P. F. F. Rosa, "Sensor fusion with cointegration analysis for IMU in a simulated fixed-wing UAV," 2017 International Conference on Military Technologies (ICMT), Brno, 2017, pp. 493-499.

[13] A. Sel, U. Güneş, Ö. Elbir and C. Kasnakoğlu, "Comparative analysis of performance of the SEPIC converter using LQR and PID controllers," 2017 21st International Conference on System Theory, Control and Computing (ICSTCC), Sinaia, 2017, pp. 839-844.

[14] R. R. Arany and A. I. Bratcu, "Robust control of a single-ended primary-inductor converter (SEPIC)," 2017 5th International Symposium on Electrical and Electronics Engineering (ISEEE), Galati, 2017, pp. 1-6.

[15] M. Ahsan, K. Shafique, A. B. Mansoor and M. Mushtaq, "Performance comparison of two altitude-control algorithms for a fixed-wing UAV," 2013 3rd IEEE International Conference on Computer, Control and Communication (IC4), Karachi, 2013, pp. 1-5.

[16] K. S. Mehta, K. Kumar and R. B. Jagadeeshchandra, "Six-DoF UAV simulation using wind tunnel test data and its cruise mode autopilot design," 2014 International Conference on Control, Instrumentation, Communication and Computational Technologies (ICCICCT), Kanyakumari, 2014, pp. 515-520.

[17] M. Laila, B. M. Houda and N. A. Said, "Comparative analysis of first order and second order discrete sliding mode control for non-minimum phase systems," 2017 18th International Conference on Sciences and Techniques of Automatic Control and Computer Engineering (STA), Monastir, 2017, pp. 647-651.

[18] M. Laila, B. M. Houda and N. A. Said, "Comparative analysis of first order and second order discrete sliding mode control for non-minimum phase systems," 2017 18th International Conference on Sciences and Techniques of Automatic Control and Computer Engineering (STA), Monastir, 2017, pp. 647-651.

[19] N. O. Lai, C. Edwards and S. K. Spurgeon, "On Output Tracking Using Dynamic Output Feedback Discrete-Time Sliding-Mode Controllers," in IEEE Transactions on Automatic Control, vol. 52, no. 10, pp. 1975-1981, Oct. 2007.

[20] H. Sira-Ramirez, "Sliding motions in bilinear switched networks," in *IEEE Transactions on Circuits and Systems*, vol. 34, no. 8, pp. 919-933, Aug 1987.

[21] S. Govindaswamy, T. Floquet and S. K. Spurgeon, "Linear matrix inequality based static output feedback sliding mode control for discrete time systems," 2009 European Control Conference (ECC), Budapest, 2009, pp. 2722-2727.

[22] H. Sira-Ramirez, "A general canonical form for sliding mode control of nonlinear systems," 1999 European Control Conference (ECC), Karlsruhe, 1999, pp. 3792-3797.

[23] N. O. Lai, C. Edwards and S. K. Spurgeon, "Discrete output feedback sliding mode based tracking control," 2004 43rd IEEE Conference on Decision and Control (CDC) (IEEE Cat. No.04CH37601), 2004, pp. 237-242 Vol.1.

[24] C. Edwards, G. Herrmann, B. Hredzak, V. Venkataramanan and S. K. Spurgeon, "A discrete-time sliding mode scheme with constrained inputs," *2007 46th IEEE Conference on Decision and Control*, New Orleans, LA, 2007, pp. 3023-3028.

[25] Nai One La, C. Edwards and S. K. Spurgeon, "An implementation of an output tracking dynamic discrete-time sliding mode controller on an aircraft simulator," International Workshop on Variable Structure Systems, 2006. VSS'06., Alghero, Sardinia, 2006, pp. 35-40.